Syntheses, Electronic Absorption, Emission, and Ion-Binding Studies of Platinum(II) C^N^C and Terpyridyl Complexes Containing Crown Ether Pendants

Vivian Wing-Wah Yam,* Rowena Pui-Ling Tang, Keith Man-Chung Wong, Xiao-Xia Lu, Kung-Kai Cheung, and Nianyong Zhu[a]

Abstract: A series of platinum(II) C^N^C complexes, [Pt(C^N^C)(L)] (HC^N^CH = 2,6-diphenylpyridine (dppy); L = Ph_2PB15C5 (**1**, B15C5 = benzo[15]crown-5), Ph_2PDMP (**2**, DMP = 3,4-dimethoxyphenyl), pyCOA15C5 (**3**, A15C5 = aza[15]crown-5), pyCON-$(CH_2CH_2OCH_3)_2$ (**4**), pyC≡CB15C5 (**5**), pyC≡CDMP (**6**)) and terpyridyl complexes, $[Pt(trpy)(L)](X)_2$ (trpy = 2,2′:6′,2″-terpyridine; L = Ph_2PB15C5, X = OTf (**7a**), PF_6 (**7b**); X = PF_6, L = Ph_2PDMP (**8**), pyC≡CB15C5 (**9**), and pyC≡CDMP (**10**)) have been successfully synthesized and characterized. The structures of **1**, **3**, and **7a** have been determined by X-ray crystallography. Excitation of complexes **1**–**6** in EtOH/MeOH (4:1 v/v) glass gave high-energy structured emission bands, assigned as derived from states of metal-perturbed intraligand (IL) origin. At higher concentrations, complexes **3**–**6** each displayed an additional, structureless emission band at 600–615 nm, with complexes **5** and **6** showing an obvious increase in the intensity of this emission band when the concentration was increased further. In dichloromethane at room temperature, complexes **3**–**6** showed, in addition to the high-energy emission at 490–505 nm, an extra, broad emission band at 620–625 nm when the concentration was increased. The emission origins of the low-energy band in glass and in fluid solutions are suggested to be derived from the ground-state oligomerization or aggregation process of the complexes. In the solid state at room temperature, complexes **1**–**6** each showed a broad, unstructured emission band at 560–600 nm, which was shifted to lower energy upon cooling to 77 K. On the other hand, the terpyridyl analogues **7**–**10** displayed intense vibronic-structured intraligand (IL) emissions at 460–472 nm in butyronitrile glass at 77 K. Solid-state samples of **9** and **10** displayed strong phosphorescence upon photoexcitation at 298 K and 77 K, tentatively assigned as derived from states of $Pt(d\pi) \rightarrow \pi^*(trpy)$ ^{3}MLCT origin (MLCT = metal-to-ligand charge transfer). The ion-binding properties of complexes **5** and **9** for Na^+, Ba^{2+}, and K^+ ions have been studied by UV/Vis spectrophotometric methods, and confirmed by ESI mass spectrometric studies. The ion-binding properties for Na^+ ions have also been probed by ^{1}H NMR experiments. For the same crown ether-containing ligand and the same metal ions, the neutral cyclometalated complexes gave larger binding constants than the positively charged terpyridyl analogues.

Keywords: crown compounds · ion-binding · N ligands · platinum terpyridine

Introduction

Square-planar platinum(II) polypyridyl complexes represent an important class of compounds that possess a rich range of spectroscopic and photophysical properties.[1–3] Of particular interest is the rather common occurrence of weak intermolecular metal–metal interactions and ligand π–π interactions in these complexes.[3, 4] In particular, platinum(II) derivatives of terpyridine have received much attention because of their rich spectroscopic behavior and useful biological properties, such as interaction with biomolecules such as DNA and proteins.[5] In recent years there has been a growing interest in the design and study of their cyclometalated counterparts,

[a] Prof. Dr. V. W.-W. Yam, R. P.-L. Tang, Dr. K. M.-C. Wong, Dr. X.-X. Lu, Dr. K.-K. Cheung, Dr. N. Zhu
Department of Chemistry, HKU–CAS Joint Laboratory of New Materials, and Open Laboratory of Chemical Biology of The Institute of Molecular Technology for Drug Discovery and Synthesis[+]
The University of Hong Kong, Pokfulam Road
Hong Kong SAR (People's Republic of China)
Fax: (852) 2857-1586
E-mail: wwyam@hku.hk

[+] Area of Excellence Scheme, University Grants Committee (Hong Kong).

Supporting information for this article is available on the WWW under http://www.chemeurj.org/ or from the author.

  0947-6539/02/0817-4066 $ 20.00+.50/0

which have also been shown to display rich photophysical and photochemical properties,[6–8] and a number of these complexes exhibit $\pi-\pi$ interactions between the cyclometalated ligands.[6c,d, 7–9] Square-planar cyclometalated Pt^{II} and Pd^{II} complexes with the general formula [M(C^N^C)(L)] (M = Pt, Pd; L = Et_2S, pyridine, pyrazine) were first reported by von Zelewsky and co-workers.[6a,b] Recent work by Rourke and co-workers has provided a versatile synthetic route to Pt(C^N^C) complexes in high yields.[10] The photophysical behavior of a number of Pt(C^N^C) complexes has also been studied by Che and co-workers;[6d] a correlation of $\pi-\pi$ interactions with luminescence properties has also been presented.[6d] Recently, we have extended our interest in the search for chemosensors[11] to the utilization of the platinum(II) terpyridyl moiety for the design of metal ion probes, and the ion-binding studies of platinum(II) terpyridyl complexes containing mercaptobenzo[15]crown-5[12] and ethynylbenzo[15]crown-5 ligands[2e] were reported. As part of our continuing effort, we are interested in extending our work to the Pt(C^N^C) moiety, which—unlike the Pt(trpy) moiety—is uncharged and may give rise to stronger ion-binding affinities for metal ions. A comparative study between the Pt(C^N^C) and the Pt(trpy) complexes would enable systematic comparison of their electronic absorption, emission, and ion-binding properties to be made, and provide insight into their spectroscopic origins. Here we report the syntheses and the electronic absorption, emission, and ion-binding properties of platinum(II) C^N^C and terpyridyl complexes with P- and N-donor crown ether pendants [Pt(C^N^C)(L)] (HC^N^CH = 2,6-diphenylpyridine (dppy); L = Ph_2PB15C5 (**1**, B15C5 = benzo[15]crown-5), Ph_2PDMP (**2**, DMP = 3,4-dimethoxyphenyl), pyCOA15C5 (**3**), pyCON($CH_2CH_2OCH_3$)$_2$ (**4**), pyC≡CB15C5 (**5**), pyC≡CDMP (**6**)) and [Pt(trpy)(L)](X)$_2$ (trpy = 2,2′:6′,2″-terpyridine; L = Ph_2PB15C5, X = OTf (**7a**), PF_6 (**7b**); X = PF_6, L = Ph_2PDMP (**8**), pyC≡CB15C5 (**9**) and pyC≡CDMP (**10**)). The X-ray crystal structures of [Pt(C^N^C)(Ph_2PB15C5)] (**1**), [Pt(C^N^C)(pyCOA15C5)] (**3**), and [Pt(trpy)(Ph_2PB15C5)](OTf)$_2$ (**7a**) have also been determined.

Results and Discussion

Syntheses and characterization: The synthetic routes to complexes **1**–**10** are summarized in Scheme 1. Both [Pt(C^N^C)(dmso)] and [Pt(trpy)(MeCN)](OTf)$_2$ serve as good precursors for ligand-substitution reactions with the appropriate N- and P-donor ligands, owing to the presence of the labile dmso and MeCN groups. Treatment of [Pt(C^N^C)(dmso)] with Ph_2PB15C5, pyCOA15C5, and

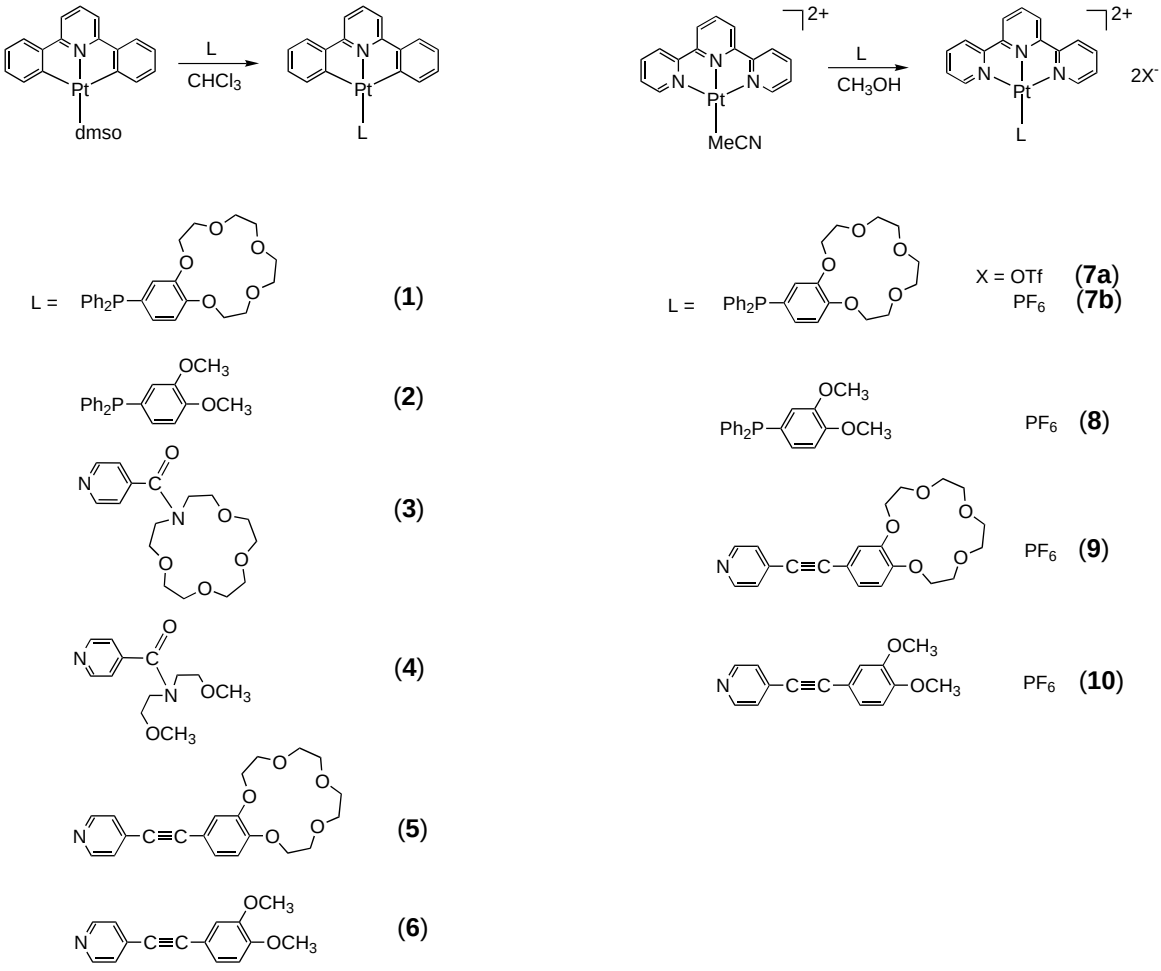

Scheme 1. Synthetic routes to complexes **1**–**10**.

  0947-6539/02/0817-4067 $ 20.00+.50/0

pyC≡CB15C5 in chloroform at room temperature afforded **1**, **3**, and **5** as air-stable, yellow to orange crystals in high yields. The crown-free analogues **2**, **4**, and **6** were also synthesized in a similar manner. Treatment of $[Pt(trpy)(MeCN)](OTf)_2$ with $Ph_2PB15C5$ and pyC≡CB15C5 in acetone, followed by metathesis with nBu_4NPF_6 and subsequent recrystallization from layering of *n*-hexane onto acetone solutions of the respective complexes, afforded **7b** and **9** as pale orange crystals in good yields. Under similar conditions, their crown-free analogues **8** and **10** were also successfully synthesized. The $^{31}P\{^1H\}$ NMR spectra of complexes **1**, **2**, **7b**, and **8** each show one sharp signal with ^{195}Pt satellites. The P–Pt coupling constants are about 4080 Hz for **1** and **2** and about 3625 Hz for **7b** and **8**, respectively, comparable to those found in the related $[Pt(C^N^C)(PPh_3)]$[6d] and $[Pt(C^N^N)(PPh_3)]ClO_4$.[7a]

The identities of all the complexes were fully established by ^1H HMR spectroscopy, IR spectroscopy, satisfactory elemental analyses, and FAB and ESI mass spectrometry. The crystal structures of $[Pt(C^N^C)(Ph_2PB15C5)]$ (**1**), $[Pt(C^N^C)(pyCOA15C5)]$ (**3**), and $[Pt(trpy)(Ph_2PB15C5)](OTf)_2$ (**7a**) have also been determined.

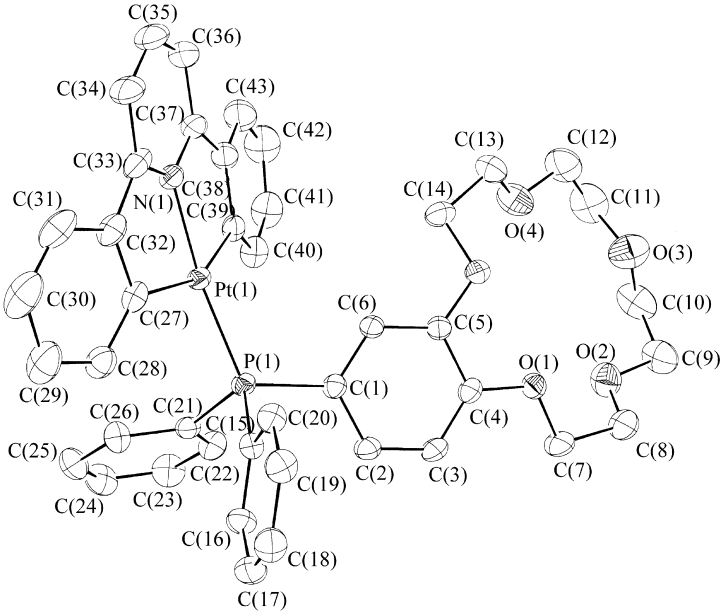

Figure 1. Structure of complex **1** (thermal ellipsoids are shown at the 30% probability level).

Crystal structure determination: Perspective drawings of **1**, **3**, and the complex cation of **7a**, with their atomic numbering schemes, are depicted in Figure 1, Figure 2, and Figure 3, respectively. The crystallographic data are given in Table 1, while selected bond lengths and bond angles are listed in Table 2. The coordination geometries of **1**, **3**, and **7a** are essentially distorted square-planar, with bond parameters similar to those observed in typical platinum(II) C^N^C tridentate and platinum(II) terpyridyl complexes.[2a,b,e, 3g,h, 6c,d, 13] Not surprisingly, the angles between the *trans* aryl carbon atoms (C(27)-Pt(1)-C(39)) deviate from the idealized value of 180° because of the orientation of the donor atoms imposed by the C^N^C ligands, which evidently restrict the bite angle. This has also commonly been observed in the related platinum(II) terpyridyl complexes.[2a,b,e, 3g,h] For complexes **1** and **7a**, the Pt–P distances are 2.23 and 2.29 Å, respectively, comparable to those found in $[Pt(C^N^C)(PPh_3)]$[6d] and $[Pt(C^N^N)(PPh_3)]ClO_4$.[7a] In complex **3**, the angles subtended at the amido-carbon atom

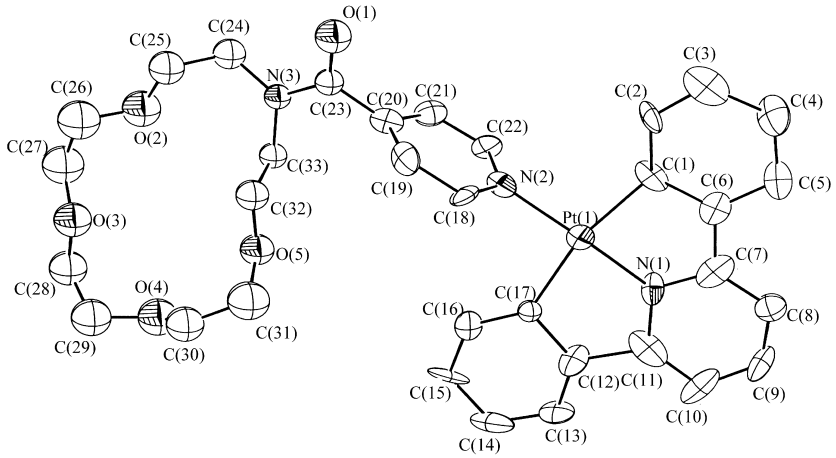

Figure 2. Structure of complex **3** (thermal ellipsoids are shown at the 30% probability level).

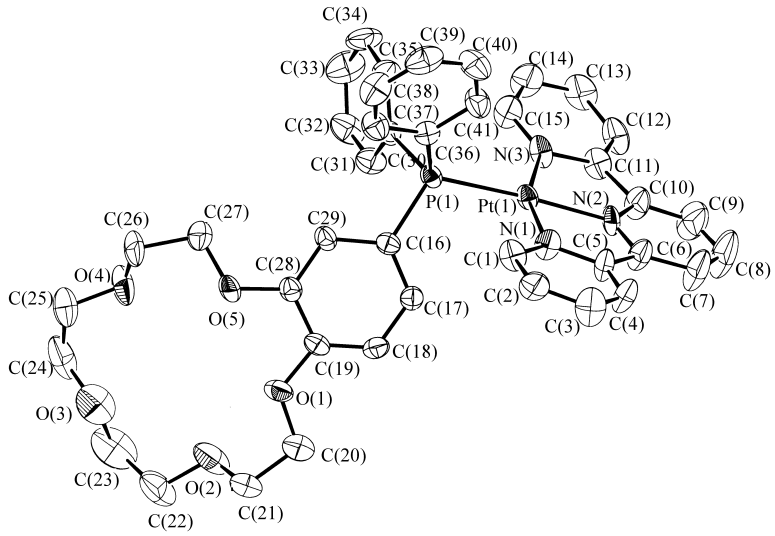

Figure 3. Structure of the complex cation of **7a** (thermal ellipsoids are shown at the 40% probability level).

0947-6539/02/0817-4068 $ 20.00+.50/0 *Chem. Eur. J.* **2002**, *8*, No. 17

Table 1. Crystal and structure determination data for **1**, **3**, and **7a**.

	1	**3**	**7a**
empirical formula	$[C_{43}H_{40}NO_5PPt]\cdot CH_2Cl_2$	$[C_{33}H_{35}N_3O_5Pt]$	$[C_{41}H_{40}N_3O_5PPt](CF_3SO_3)_2\cdot 2(CH_3)_2CO$
formula weight	961.75	748.73	1295.14
temperature [K]	301	301	301
crystal system	triclinic	monoclinic	monoclinic
space group	$P\bar{1}$ (no. 2)	$P2_1$	$C2/c$ (no. 15)
a [Å]	9.114(1)	9.507(2)	31.541(4)
b [Å]	20.627(2)	33.605(7)	17.658(4)
c [Å]	22.024(2)	9.524(2)	24.072(4)
α [°]	83.56(1)	90	90
β [°]	82.70(1)	94.51(3)	121.495(6)
γ [°]	88.67(1)	90	90
volume (Å^3)	4080.7(7)	3033.3(10)	11431(3)
crystal color	yellow	orange	orange
Z	4	4	8
$F(000)$	1920	1488	5200
ρ [g cm^{-3}]	1.565	1.640	1.505
crystal size [mm]	$0.50\times0.40\times0.20$	$0.50\times0.20\times0.10$	$0.30\times0.15\times0.10$
μ [mm^{-1}]	3.654	4.671	2.626
collection range [°]			
$2\theta_{max}$	51.10	47.68	50
	$-10\le h\le 9$	$-10\le h\le 10$	$0\le h\le 37$
	$-24\le k\le 24$	$-36\le k\le 36$	$0\le k\le 20$
	$-24\le l\le 26$	$-9\le l\le 9$	$-28\le l\le 24$
no. of data collected	23004	9662	10628
no. of unique data	13904	5761	10420
no. of data used in refinement	13904	5761	6331
no. of parameters refined	973	583	566
goodness-of-fit on F^2	1.131	0.971	2.91
final R indices R,[a] wR[b]	0.0371, 0.0988	0.0485, 0.1112	0.072, 0.103
maximum shift, $(\Delta/\sigma)_{max}$	0.007	0.001	0.06
largest diff. peak and hole [eÅ^{-3}]	0.761, −2.390	0.920, −1.177	1.53, −1.61

[a] $R=\Sigma||F_o|-|F_c||/\Sigma|F_o|$. [b] $wR=\{\Sigma[w(F_o^2-F_c^2)^2]/\Sigma[w(F_o^2)^2]\}^{1/2}$.

C(23) (117°–124°) are typically those of sp^2 hybridization. The plane of the pyridine ring of the pyCOA15C5 ligand is almost orthogonal to that of the Pt(C^N^C) moiety, with a dihedral angle of 70.10°. The Pt–N bond length is 2.04 Å, which is in good agreement with the values of 2.04 and 2.03 Å for [Pt(C^N^C)(*t*Bupy)][6d] and [Pt(C^N^N)(py)]ClO_4,[7c] respectively. Neither short Pt···Pt contacts nor significant π–π interactions were observed in the crystal lattices of **1**, **3**, and **7a**, probably because of the steric bulk of the Ph_2PB15C5 and pyCOA15C5 ligands.

Electronic absorption spectroscopy: The electronic absorption spectra of complexes **1**–**6** show intense vibronic-structured absorption bands at 334–364 nm ($\varepsilon>10^4$ dm^3 mol^{-1} cm^{-1}) with vibrational progressional spacings of about 1300 cm^{-1}, corresponding to the skeletal vibrational frequency of the C^N^C ligand. In addition, a shoulder at 416–482 nm ($\varepsilon=420-650$ dm^{3}mol^{-1}cm^{-1}) and a weak band at 508–512 nm ($\varepsilon=40-230$ dm^{3}mol^{-1}cm^{-1}) are observed. The electronic absorption data for complexes **1**–**10** are summarized in Table 3. Figure 4 shows the electronic absorption spectrum of complex **3** in dichloromethane at room temperature. With reference to previous reports on platinum(II) C^N^C tridentate complexes,[6d] the high-energy bands are tentatively assigned to the metal-perturbed intraligand (IL) transitions of the C^N^C ligand, while the shoulders are assigned as $d\pi(Pt)\rightarrow\pi^*$(C^N^C) metal-to-ligand charge transfer (MLCT) transitions. The low-energy weak absorption bands at 508–512 nm are unlikely to be d–d transitions, since the C^N^C ligand is a strong σ donor and it is unlikely that they would occur at such low energies. Instead, a spin-forbidden $^3\pi-\pi^*$(C^N^C) intraligand transition is suggested, in view of the large spin–orbit coupling resulting from the presence of the heavy Pt atom. A similar assignment of a $^3\pi-\pi^*$(ppy) has also been suggested for an absorption at similar energies for the related $[Rh(ppy)_2(bpy)]PF_6$ and $[Ir(ppy)_2(bpy)]PF_6$ (ppyH = 2-phenylpyridine, bpy = 2,2′-bipyridine).[14] All the complexes were found to obey Beer's Law in the concentration range of $10^{-5}-10^{-2}$ mol dm^{-3}. On the other

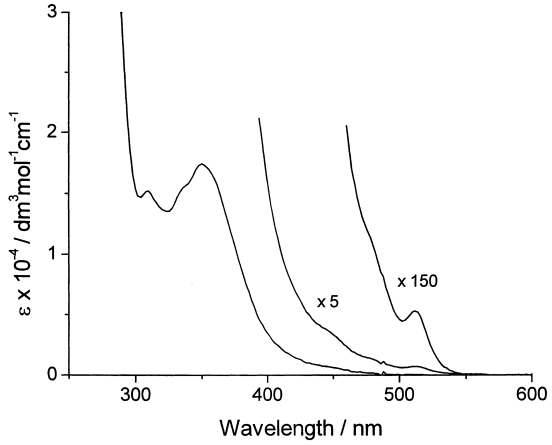

Figure 4. Electronic absorption spectrum of **3** in dichloromethane at room temperature.

Table 2. Selected bond lengths [Å] and bond angles [°] for **1**, **3**, and **7a**.

		1	
Pt(1)–N(1)	2.033(4)	C(27)-Pt(1)-N(1)	79.41(19)
Pt(1)–C(27)	2.083(5)	N(1)-Pt(1)-C(39)	80.07(19)
Pt(1)–C(39)	2.082(5)	C(27)-Pt(1)-C(39)	157.24(19)
Pt(1)–P(1)	2.2268(11)	C(27)-Pt(1)-P(1)	101.04(14)
P(1)–C(15)	1.815(5)	N(1)-Pt(1)-P(1)	171.98(11)
P(1)–C(21)	1.826(5)	C(39)-Pt(1)-P(1)	100.66(14)
P(1)–C(1)	1.830(4)	Pt(1)-P(1)-C(1)	115.9(15)
		Pt(1)-P(1)-C(21)	111.15(15)
		Pt(1)-P(1)-C(15)	115.31(15)
		C(15)-P(1)-C(21)	106.0(2)
		C(21)-P(1)-C(1)	106.6(2)
		C(15)-P(1)-C(1)	100.9(2)
		3	
Pt(1)–N(1)	1.918(16)	C(1)-Pt(1)-N(1)	83.0(10)
Pt(1)–N(2)	2.09(2)	N(1)-Pt(1)-C(17)	82.6(8)
Pt(1)–C(1)	2.08(2)	C(1)-Pt(1)-C(17)	165.6(9)
Pt(1)–C(17)	2.024(18)	C(1)-Pt(1)-N(2)	97.8(9)
		N(1)-Pt(1)-N(2)	176.7(8)
		C(17)-Pt(1)-N(2)	96.6(7)
		C(20)-C(23)-N(3)	119(2)
		C(23)-N(3)-C(24)	118.6(19)
		C(23)-N(3)-C(33)	121.7(18)
		7a	
Pt(1)–N(1)	2.07(1)	N(1)-Pt(1)-N(2)	79.8(5)
Pt(1)–N(2)	2.00(1)	N(2)-Pt(1)-N(3)	79.5(5)
Pt(1)–N(3)	2.097(10)	N(1)-Pt(1)-N(3)	158.7(5)
Pt(1)–P(1)	2.287(3)	N(1)-Pt(1)-P(1)	97.9(3)
P(1)–C(16)	1.81(1)	N(2)-Pt(1)-P(1)	176.6(3)
P(1)–C(30)	1.82(1)	N(3)-Pt(1)-P(1)	103.0(3)
P(1)–C(36)	1.81(1)	Pt(1)-P(1)-C(16)	111.1(5)
		Pt(1)-P(1)-C(30)	117.1(4)
		Pt(1)-P(1)-C(36)	110.0(5)
		C(16)-P(1)-C(30)	102.5(6)
		C(30)-P(1)-C(36)	104.1(6)
		C(16)-P(1)-C(36)	111.8(6)
		P(1)-C(16)-C(29)	118.4(10)
		P(1)-C(16)-C(17)	122(1)

hand, the electronic absorption spectra of complexes **7**–**10** show vibronic-structured bands at 290–340 nm ($\varepsilon > 10^4$ dm^3 mol^{-1} cm^{-1}), characteristic of the intraligand (IL) transition of the terpyridine ligand, and a shoulder at 368–390 nm ($\varepsilon = 1900-8440$ dm^3 mol^{-1} cm^{-1}). With reference to previous spectroscopic studies on platinum(II) terpyridyl and tri-*tert*-butyl-terpyridyl complexes,[2a,d,e, 3g,h] the low-energy band at 368–390 nm is assigned as the $d\pi(Pt) \rightarrow \pi^*$(trpy) MLCT transition.

Emission properties: All the complexes were found to exhibit luminescence at 77 K in alcoholic or butyronitrile glasses, while only **3**–**6** showed emission properties in dichloromethane solutions at room temperature. The photophysical data are collected in Table 3. The large Stokes' shifts and the observed emission lifetimes in the microsecond range are suggestive of a triplet parentage. In EtOH/MeOH (4:1 v/v) glass at 77 K and at low concentrations (5×10^{-7} mol dm^{-3}), complexes **1**–**6** all show highly structured emission bands at 506–513 nm with vibrational progressional spacings of about 1300 cm^{-1}, typical of the aromatic vibrational mode of the C^N^C ligand. These emissions, which are also observed in the related Pt(C^N^C) and Au(C^N^C) complexes,[6c,d] are tentatively assigned as derived from states of metal-perturbed $^3\pi-\pi^*$(C^N^C) origin. With increasing concentration, complexes **3**–**6** each show, in addition to the vibronic-structured emission, a broad emission band centered at 600–615 nm, with complexes **5** and **6** showing an obvious preferential enhancement in the emission intensity of this band at 615 nm with increasing concentration from 5×10^{-7} to 5×10^{-5} mol dm^{-3} (Figure 5a). In contrast, complexes **1** and **2** did not show such behavior with increasing concentration up to 5×10^{-3} mol dm^{-3}. The excitation spectra monitored at 508 nm and 615 nm appeared different, indicating that the two emission bands were of different origins and that the broad emission bands at about 600–615 nm were unlikely to be due to excimeric emissions (Figure 5b). It is likely that the unstructured bands at 600–615 nm originate from emissive states resulting from ground-state aggregation or oligomerization of the complexes either through $\pi-\pi$ interaction of the cyclometalated ligands or metal$\cdots$metal interactions. This may further be supported by the less obvious or the absence of low-energy emissions in complexes **3**–**4** and **1**–**2**, respectively, in which the pyridine-amide and the phosphine ligands are sterically more bulky than the pyridine-acetylide ligand, rendering aggregation less favorable relative to complexes **5** and **6**. Although all the complexes appeared to obey Beer's Law in their electronic absorption at room temperature, one could not totally exclude the possibility of a ground-state aggregation process since the association constants may be too small to be observable in the UV-Vis absorption spectra. Interestingly, in dichloromethane at room temperature, complexes **3**–**6** also showed a high-energy emission band at 490–505 nm in the concentration range $5 \times 10^{-7}-5 \times 10^{-6}$ mol dm^{-3}, while upon increasing the concentration to 5×10^{-5} mol dm^{-3}, a lower-energy broad band at 620–625 nm appeared. This low-energy emission band at 620–625 nm, which only appeared at higher concentration, is also thought to arise from states derived from ground-state aggregated species. The appearance of this band above concentrations of 10^{-5} mol dm^{-3} in dichloromethane at 298 K, as compared to above 10^{-7} mol dm^{-3} in 77 K glass, is suggestive of a larger

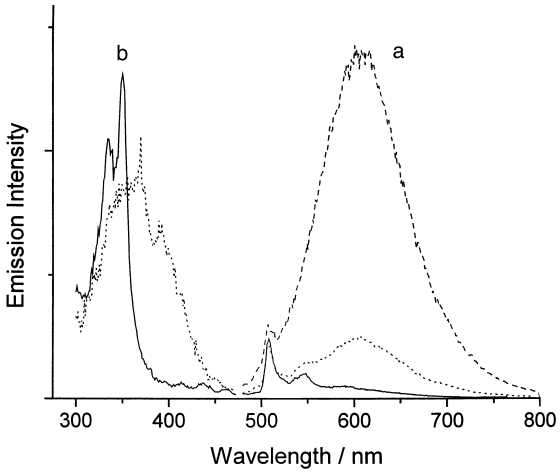

Figure 5. a) Emission spectra of **5** at concentrations of 5×10^{-7} (——), 5×10^{-6} (···), and 5×10^{-5} mol dm^{-3} (----) in EtOH/MeOH (4:1 v/v) glass at 77 K. b) Excitation spectra monitored at 508 nm (——) and 615 nm (···) in EtOH/MeOH (4:1 v/v) glass at 77 K.

0947-6539/02/0817-4070 $ 20.00+.50/0 *Chem. Eur. J.* **2002**, *8*, No. 17

Table 3. Photophysical spectral data for **1**—**10**.

Complex	Absorption[a] λ_{abs} [nm] (ε [$dm^3 mol^{-1} cm^{-1}$])	Emission medium (T/K)	λ_{em} [nm] (τ_o [μs[b]])
1	252 (50550), 282 (43030), 338sh (14630), 352 (16970), 416 (490), 436sh (420), 508 (40)	CH_2Cl_2 (298)	–[c]
		solid (298)	570 (0.9)
		solid (77)	600 (8.2)
		glass[d] (77)	513 (13.3)
2	254 (49180), 282 (42090), 336sh (13870), 352 (16800), 416 (490), 438sh (420), 508 (50)	CH_2Cl_2 (298)	–[c]
		solid (298)	560 (1.1)
		solid (77)	575 (7.6)
		glass[d] (77)	512 (12.1)
3	256 (45450), 280 (46090), 334sh (14500), 350 (16070), 446sh (650), 512 (110)	CH_2Cl_2[e] (298)	505 (2.7), 625 (1.1)
		solid (298)	580 (0.1)
		solid (77)	600 (4.2)
		glass[d] (77)	506 (20.9) 600 (6.0)
4	254 (43690), 282 (42150), 334sh (16870), 350 (16085), 448sh (540), 512 (100)	CH_2Cl_2[e] (298)	505 (2.8), 620 (1.4)
		solid (298)	585 (0.1)
		solid (77)	600 (4.8)
		glass[d] (77)	506 (21.6), 610 (4.8)
5	256 (49730), 280 (43590), 334sh (14530), 360 (35730), 480sh (613), 512 (220)	CH_2Cl_2[e] (298)	490 (2.4), 625 (1.7)
		solid (298)	600 (0.1)
		solid (77)	620 (2.2)
		glass[d] (77)	508 (250.6), 615 (3.6)
6	256 (45055), 282 (38240), 334sh (15760), 364 (30360), 482sh (470), 512 (230)	CH_2Cl_2[e] (298)	495 (2.6), 620 (1.8)
		solid (298)	600 (0.2)
		solid (77)	615 (2.6)
		glass[d] (77)	508 (234.9), 615 (3.8)
7	274 (26530), 296 (16950), 326sh (10440), 340 (12160), 370sh (3200), 390 (1990)	CH_3CN (298)	–[c]
		solid (298)	–[c]
		solid (77)	465 (11.7)
		glass[f] (77)	460 (38.6)
8	276 (28710), 290 (18020), 326sh (11130), 340 (12100), 370sh (3670), 390 (2260)	CH_3CN (298)	–[c]
		solid (298)	–[c]
		solid (77)	465 (9.9)
		glass[f] (77)	465 (37.7)
9	244 (46650), 282 (33715), 310sh (31015), 326 (31965), 340 (22190), 370sh (8440), 390sh (4210)	CH_3CN (298)	440 (2.2)
		solid (298)	580 (0.1)
		solid (77)	555 (13.9)
		glass[f] (77)	470 (11.6)
10	244 (47655), 282 (34630), 312sh (28655), 326 (33520), 340 (19950), 368sh (7430), 390sh (3650)	CH_3CN (298)	440 (2.1)
		solid (298)	585 (0.1)
		solid (77)	555 (15.6)
		glass[f] (77)	472 (19.7)

[a] In dichloromethane for **1**–**6;** in acetonitrile for **7b**–**10** at 298 K. [b] τ_0 is the lifetime at infinite dilution. [c] Non-emissive. [d] In EtOH/MeOH (4:1 v/v) glass (concentration = 5×10^{-7}–5×10^{-5} mol dm^{-3}). [e] Concentration = 5×10^{-7}–5×10^{-5} mol dm^{-3}. [f] In butyronitrile glass (concentration = 5×10^{-6}; mol dm^{-3}).

association constant for the aggregation process at low temperature than at room temperature, in line with what one would have expected. Complexes **1**–**6** show bright luminescence at 560–600 nm in the solid state at room temperature, at similar energies to the low-energy emission in 77 K glass. Upon cooling to 77 K, the emission maxima are red-shifted to 575–620 nm with reduced bandwidths. This may be attributed to a lattice contraction of the solid sample at low temperature. Figure 6 shows the solid-state emission spectra of **3** at 298 and 77 K. The emission energies in solution and in the solid state compare well to the 77 K alcoholic glass emissions at 615 nm for **5** and **6**, and are therefore similarly assigned as originating from ground-state aggregation or oligomerization of the complexes.

Complexes **7**–**10** all show emission properties in butyronitrile glass at 77 K, while complexes **9** and **10** display a high-energy emission at 440 nm in acetonitrile at 298 K, attributed

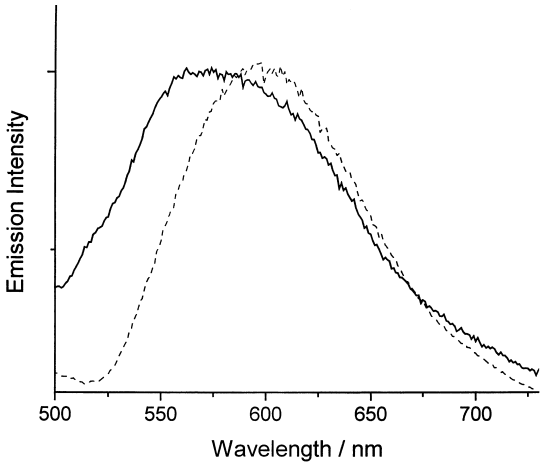

Figure 6. Solid-state emission spectra of **3** at 298 K (——) and 77 K (- - - -).

  0947-6539/02/0817-4071 $ 20.00+.50/0

to the metal-perturbed ligand center phosphorescence. The emission spectra of **7**–**10** in butyronitrile glass at 77 K show a vibronic-structured band at 460–472 nm with progressional spacings of about 1300 cm^{-1}, typical of the skeletal vibrational frequency of the terpyridine ligand (Figure 7). Complexes **9**

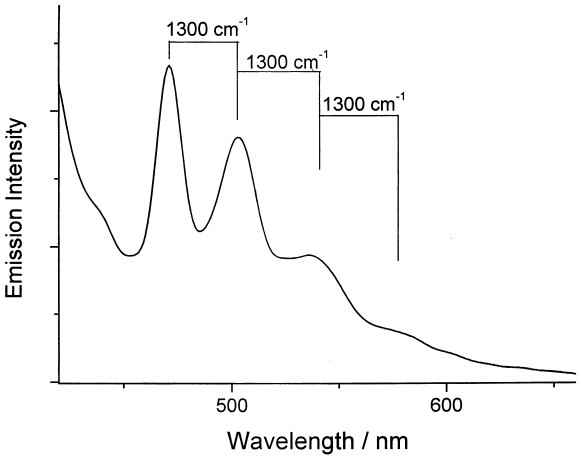

Figure 7. Emission spectrum of **9** in butyronitrile glass at 77 K.

and **10**, unlike their C^N^C analogues **5** and **6**, show no emission bands at about 615 nm with increasing concentration of the complex either in solution state or in butyronitrile glass at 77 K. It is likely that complexes **9** and **10**, which bear overall positive charges of +2, do not favor the oligomerization process. Complexes **9** and **10** display luminescence at 580–585 nm in the solid state at room temperature. With reference to previous spectroscopic studies on related platinum(II) terpyridyl complexes,[2a, 3e,g,h] the emission is tentatively assigned as originating from a $d\pi(Pt) \rightarrow \pi^*(trpy)$ ^{3}MLCT state.

Cation-binding properties: Of all the complexes studied, only **5** and **9** show a UV/Vis spectral change upon addition of alkali and alkaline earth metal cations, while the other complexes, including **1**, **3**, and **7**, which contain the $Ph_2PB15C5$ or pyCOA15C5 ligand, give either no or little observable UV/Vis spectral change. Figure 8 and Figure 9 show the UV/Vis

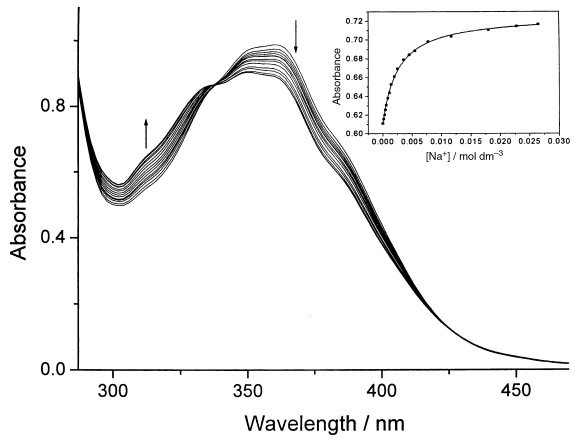

Figure 8. Electronic absorption spectral traces of **5** (3×10^{-5} mol dm^{-3}) in CH_2Cl_2/MeOH (1:1 v/v) (0.1 mol dm^{-3} nBu$_4$NPF$_6$) upon addition of $NaClO_4$ (path length = 1 cm). The insert shows a plot of absorbance against [Na^+], monitored at $\lambda = 320$ nm (■) and its theoretical fit (——).

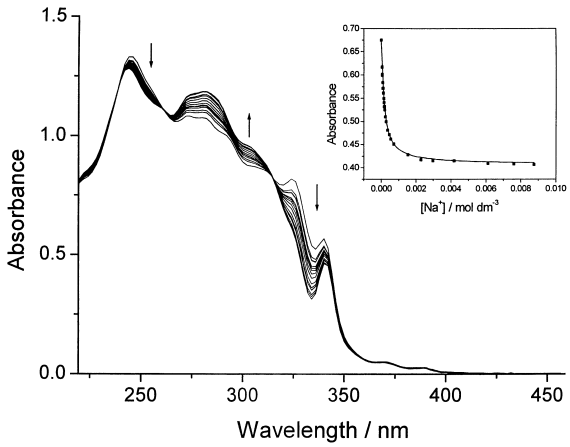

Figure 9. Electronic absorption spectral traces of **9** (2.5×10^{-5} mol dm^{-3}) in CH_3CN (0.1 mol dm^{-3} nBu$_4$NPF$_6$) upon addition of $NaClO_4$ (path length = 1 cm). The insert shows a plot of absorbance against [Na^+] monitored at $\lambda = 320$ nm (■) and its theoretical fit (——).

absorption spectral traces of **5** and **9**, respectively, upon addition of sodium perchlorate, with well-defined isosbestic points. Spectrochemical recognition of guest metal ions is confirmed by the absence of spectral changes in the electronic absorption spectra of the respective control complexes **6** and **10**. In the binding studies of **5**, two solvent systems, CH_2Cl_2/MeOH (1:1 v/v) and CH_3CN/DMF (8:2 v/v), were used. In the cases of Na^+ and Ba^{2+} ion-binding in CH_2Cl_2/MeOH (1:1 v/v), isosbestic points, indicative of a clean reaction, were observed at 340 and 338 nm, respectively. The close resemblance of the experimental data to the theoretical fits according to Equation (1) (see Experimental Section) is supportive of a 1:1 complexation model (Figure 8 insert), and was further confirmed by the method of continuous variation, in which a break point was observed at a mole fraction **5**/(**5** + Na^+) of 0.5. Log K_s values of 3.29(±0.01) and 2.74(±0.01) for Na^+ and Ba^{2+} ion-binding were obtained in CH_2Cl_2/MeOH (1:1 v/v), while these values decreased to 2.59(±0.01) and 1.90(±0.02), respectively, in CH_3CN/DMF (8:2 v/v). The difference may be attributable to the difference in the polarity of the solvent, in which the metal cations are already well solvated or stabilized by the more polar solvent molecules (DMF), making cation binding into the crown cavity less favored. Similar findings have also recently been reported for the related [Pt(trpy)(S-benzo[15]crown-5)]PF_6 and [Pt(trpy)(C≡C-benzo[15]crown-5)]PF_6.[2e, 12] For KPF_6, due to its low solubility in CH_2Cl_2/MeOH (1:1 v/v), only CH_3CN/DMF (8:2 v/v) was employed for the binding studies. The lack of well-defined isosbestic points, as well as the good agreement of the experimental data to the theoretical fits of Equation (2) (see Experimental Section) in Figure 10, suggest the formation of two complexes of stoichiometries 2:1 (**5**:K^+) and 1:1, with log K_{11} and log K_{21} values of 2.73 (±0.05) and 3.34 (±0.05), respectively, probably as a result of the tendency for K^+ ions to bind in a 2:1 sandwich mode to benzo[15]crown-5, which has a cavity size smaller than the size of the K^+ ion. A similar model has also been observed for the binding of K^+ ions to [Pt(trpy)(S-benzo[15]crown-5)]PF_6 and [Pt(trpy)(C≡C-benzo[15]crown-5)]PF_6.[2e, 12]

0947-6539/02/0817-4072 $ 20.00+.50/0 *Chem. Eur. J.* **2002**, *8*, No. 17

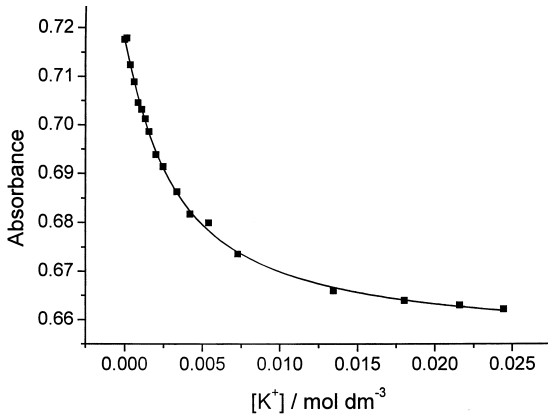

Figure 10. Plot of absorbance of **5** (3×10^{-5} mol dm^{-3}) in CH_3CN/DMF (8:2 v/v) (0.1 mol dm^{-3} nBu$_4$NPF$_6$) against [K$^+$] monitored at $\lambda = 380$ nm (■) and its theoretical fit (——).

Similarly, complex **9** shows a 1:1 binding mode for Na^+ and a mixture of 1:1 and 2:1 binding for K^+ ions. The log K_s value obtained for Na^+ is 3.85($\pm$0.01), while log K_{11} and log K_{21} are found to be 3.40($\pm$0.02) and 3.44($\pm$0.03), respectively, for K^+ ion-binding in acetonitrile. In CH_3CN/DMF (8:2 v/v), the log K_s values for Na^+ ion-binding decreased to 2.28($\pm$0.01), while log K_{11} and log K_{21} decreased to 2.25($\pm$0.03) and 2.34($\pm$0.03), respectively. The binding constants for Na^+ and K^+ ion-binding for complex **9** are found to be smaller than those for complex **5** in CH_3CN/DMF (8:2 v/v). This is reasonable, since complex **5**, being a neutral species, should have stronger ion-binding affinities for metal ions and hence a larger binding constant.

^{1}H NMR spectroscopy has also been employed to probe the ion-binding properties of complexes **5** and **9** for Na^+ ions. The log K_s values obtained by the ^{1}H NMR method are 4.0($\pm$0.01) in CH_2Cl_2/MeOH (1:1 v/v) for **5** and 3.9($\pm$0.01) in acetonitrile for **9**, in good agreement with those determined by the UV-visible spectrophotometric method.

Positive ESI mass spectrometry provides another piece of evidence for the ion-binding properties of the complexes. Table 4 summarizes the ion cluster peaks for the ion-bound adducts of the platinum(II) crown ether containing complexes and alkali metal cations, with 1:1 adducts being observed upon addition of $NaClO_4$ or $Ba(ClO_4)_2$ to **1**, **3**, **5**, **7b**, and **9**, while with K^+ ions both 1:1 and 2:1 adducts were observed. This further confirms the complexation stoichiometry models obtained from the electronic absorption studies. Similarly to what was seen in the absorption studies, crown-free analogues do not show the presence of such ion-bound adducts upon addition of metal salts, which is supportive of the importance of the crown ether in the specific association of the complexes with the metal ions. The lack of UV/Vis absorption changes observed for the ion-binding studies in **1**, **3**, and **7**, despite the occurrence of ion-binding as reflected in the ESI-MS studies, is likely to be attributable to the poor conjugation and electronic communication of the Ph_2PB15C5 and pyCOA15C5 ligands to the platinum(II) C^N^C and terpyridyl chromophores, indicating the importance of electronic communication in the design of effective spectrochemical chemosensors.

Table 4. Ion clusters observed in the positive ESI-mass spectra of **1**, **3**, **5**, **7b**, and **9** with $NaClO_4$, KPF_6, and $Ba(ClO_4)_2$.

Complex	*m/z*	Ion cluster
1	900	[Pt(C^N^C)(Ph$_2$PB15C5)·Na]$^+$
	916	[Pt(C^N^C)(Ph$_2$PB15C5)·K]$^+$
	1792	{[Pt(C^N^C)(Ph$_2$PB15C5)]$_2$·K}$^+$
	1114	[Pt(C^N^C)(Ph$_2$PB15C5)·Ba]ClO$_4$}$^+$
3	772	[Pt(C^N^C)(pyCOA15C5)·Na]$^+$
	788	[Pt(C^N^C)(pyCOA15C5)·K]$^+$
	1537	{[Pt(C^N^C)(pyCOA15C5)]$_2$·K}$^+$
	986	{[Pt(C^N^C)(pyCOA15C5)·Ba]ClO$_4$}$^+$
5	817	[Pt(C^N^C)(pyC≡CB15C5)·Na]$^+$
	833	[Pt(C^N^C)(pyC≡CB15C5)·K]$^+$
	1627	{[Pt(C^N^C)(pyC≡CB15C5)]$_2$·K}$^+$
	1031	{[Pt(C^N^C)(pyC≡CB15C5)·Ba]ClO$_4$}$^+$
7b	1102	{[Pt(trpy)(Ph$_2$PB15C5)·Na](ClO$_4$)$_2$}$^+$
	1209	{[Pt(trpy)(Ph$_2$PB15C5)·K](PF$_6$)$_2$}$^+$
	1117	{{[Pt(trpy)(Ph$_2$PB15C5)]$_2$·K}(PF$_6$)$_3$}$^{2+}$
	1316	{[Pt(trpy)(Ph$_2$PB15C5)·Ba](ClO$_4$)$_3$}$^+$
9	1019	{[Pt(trpy)(pyC≡CB15C5)·Na](ClO$_4$)$_2$}$^+$
	1126	{[Pt(trpy)(pyC≡CB15C5)·K](PF$_6$)$_2$}$^+$
	1034	{{[Pt(trpy)(pyC≡CB15C5)]$_2$·K}(PF$_6$)$_3$}$^{2+}$
	1233	{[Pt(trpy)(pyC≡CB15C5)·Ba](ClO$_4$)$_3$}$^+$

Conclusion

A series of platinum(II) C^N^C and terpyridyl complexes with P- and N-donor crown ether ligands has been prepared and fully characterized. The electronic absorption spectra of the complexes are dominated by intraligand $\pi-\pi^*$ and metal-to-ligand charge transfer transitions. The weak absorption at 508–512 nm in the Pt(C^N^C) complexes, which is absent in the terpyridyl analogues, is tentatively assigned as a spin-forbidden $\pi-\pi^*$(C^N^C) intraligand singlet–triplet transition. All C^N^C crown complexes show highly structured bands at 506–513 nm in EtOH/MeOH glasses (4:1 v/v), which are tentatively assigned to the metal-perturbed $^3\pi-\pi^*$ states, while complexes **3**–**6** show an additional, broad, unstructured band at 600–615 nm when the concentration is increased. With the less bulky pyridine–acetylide ligands, the intensity of this low-energy band becomes enhanced as the concentration is increased. It is suggested that this emission at 600–615 nm originates from the ground-state aggregation or oligomerization of the complexes. A low-energy emission band at 620–625 nm is also observed in dichloromethane at room temperature for complexes **3**–**6**, but only at higher concentrations than used in alcoholic glass at 77 K. This can be rationalized by a larger association constant for the aggregation process at low temperature than at room temperature. Complexes **1**–**6** show bright luminescence at 560–600 nm in the solid state at room temperature, the emission maxima becoming red-shifted to 575–620 nm with reduced bandwidths upon cooling to 77 K. With the comparable energy in glass at about 615 nm, the low-energy emissions in the solid and solution states are similarly assigned. The absence of such a low-energy, structureless band in the solution state and in butyronitrile glass at 77 K in the platinum(II) terpyridyl analogues is attributed to the overall charge of +2 on the complexes, which hinders the oligomerization process as a result of strong electrostatic repulsion. It

  0947-6539/02/0817-4073 $ 20.00+.50/0

can be concluded that the aggregation or oligomerization process is influenced by both steric and Coulombic effects.

The cation-binding properties of the crown ether-containing complexes have been studied. The spectral changes upon addition of guest metal ions for complexes **5** and **9** were monitored by electronic absorption and ^{1}H NMR studies, and the stability constants were determined. Complex **5** was found to have larger binding constants than its terpyridyl analogue complex **9**. This has been attributed to the absence of charge in complex **5**, which could give rise to stronger binding affinities for metal ions. The ion-binding properties have further been confirmed by positive ESI mass spectrometry. In general, 1:1 adducts were observed for the binding of Na^+ and Ba^{2+}, while both 1:1 and 2:1 adducts were observed for K^+. The lack of UV/Visible spectral changes in **1**, **3**, and **7** upon metal ion-binding establishes the importance of electronic communication between the receptor site and the chromophoric moieties.

Experimental Section

Materials and reagents: Dichloro(1,5-cyclooctadiene)platinum(II), potassium tetrachloroplatinate(II), and 2,2′:6′,2″-terpyridine were obtained from Strem Chemicals Inc. 2,6-Diphenylpyridine was obtained from Lancaster Synthesis Ltd. Ph_2PB15C5,[15] Ph_2PDMP,[15] pyCOA15C5,[16] pyCON($CH_2CH_2OCH_3$)$_2$,[16] pyC≡CB15C5,[17] and pyC≡CDMP[17] were synthesized according to modifications of the methods described in the literature. [Pt(trpy)(MeCN)](OTf)$_2$[2b] and [Pt(C^N^C)(dmso)][10b] were synthesized according to the published procedures. All solvents were purified and distilled by standard procedures before use. All other reagents were of analytical grade and were used as received.

Physical measurements and instrumentation: UV/Vis spectra were obtained on a Hewlett–Packard 8452A diode array spectrophotometer, IR spectra as KBr disks on a Bio-Rad FTS-7 Fourier transform infrared spectrophotometer (4000–400 cm^{-1}), and steady-state excitation and emission spectra on a Spex Fluorolog 111 spectrofluorimeter. Solid-state photophysical studies were carried out with solid samples contained in a quartz tube inside a quartz-walled Dewar flask. Measurements on the alcoholic and butyronitrile glasses or solid-state samples at 77 K were conducted similarly, with a liquid nitrogen-filled optical Dewar flask. Excited state lifetimes were measured with a conventional laser system. The excitation source was the 355 nm output (third harmonic, 8 ns) of a Spectra-Physics Quanta-Ray Q-switched GCR-150 pulsed Nd-YAG laser (10 Hz).

All solutions for photophysical studies were degassed on a high-vacuum line in a two-compartment cell consisting of a 10 ml Pyrex bulb and a 1 cm path-length quartz cuvette, and sealed from the atmosphere by a Bibby Rotaflo HP6 Teflon stopper. The solutions were subject to at least four freeze–pump–thaw cycles.

^{1}H NMR (400 MHz) spectra were recorded on a Bruker DPX 400 FT-NMR spectrometer at 298 K, and chemical shifts are reported relative to Me_4Si. ^{31}P{^{1}H} NMR (162 MHz) spectra were recorded on a Bruker DPX 400 FT-NMR spectrometer, and chemical shifts are reported relative to 85% H_3PO_4. Positive-ion FAB mass spectra were recorded on a Finnigan MAT 95 mass spectrometer, and positive ESI mass spectra on a Finnigan LCQ mass spectrometer. Elemental analyses of the new complexes were performed on a Carlo Erba 1106 elemental analyzer at the Institute of Chemistry, Chinese Academy of Sciences.

The electronic absorption spectral titration for determination of binding constants was performed with a Hewlett–Packard 8452A diode array spectrophotometer at 25 °C, controlled by a Lauda RM6 compact low-temperature thermostat. Supporting electrolyte (0.1 mol dm^{-3} nBu$_4$NPF$_6$) was added to maintain a constant ionic strength of the sample solution in order to avoid any changes arising from a change in the ionic strength of the medium. Binding constants for 1:1 complexation and both 1:1 and 2:1 stoichiometries were determined by nonlinear least-squares fits to Equations (1) and (2), respectively, the derivations of which were described previously.[2e, 12]

$$X = X_0 + \frac{X_{lim} - X_0}{2[Pt]_T}\{[Pt]_T + [M^{n+}] + 1/K_s - [([Pt]_T + [M^{n+}] + 1/K_s)^2 - 4[Pt]_T[M^{n+}]]^{1/2}\} \quad (1)$$

In Equation (1) X_0 and X are the absorbance of the complex at a selected wavelength in the absence and in the presence of the metal cation, respectively, $[Pt]_T$ is the total concentration of the complex, $[M^{n+}]$ is the concentration of the metal cation M^{n+}, X_{lim} is the limiting value of absorbance in the presence of excess metal ion, and K_s is the stability constant.

$$X = \frac{X_0}{[Pt]_T}[Pt]_1 + \frac{X_{lim}}{[Pt]_T}[Pt \cdot M^{n+}] + \frac{2X_{lim}}{[Pt]_T}[Pt_2 \cdot M^{n+}] \quad (2)$$

where

$$[Pt \cdot M^{n+}] = \frac{a}{2K_{21}}$$

$$[Pt]_1 = \frac{a}{2K_{21}K_{11}[M^{n+}]}$$

$$[Pt_2 \cdot M^{n+}] = \frac{a^2}{4K_{21}K_{11}[M^{n+}]}$$

$$a = -1 - K_{11}[M^{n+}] + \sqrt{(1 + K_{11}[M^{n+}])^2 + 4K_{21}K_{11}[M^{n+}][Pt]_T}$$

where $[Pt]_1$ is the concentration of complex in the unbound state, $[PtM^{n+}]$ and $[Pt_2M^{n+}]$ are the concentrations of the 1:1 and 2:1 ion-bound adducts, respectively, and K_{11} and K_{21} are the respective stability constants for 1:1 and 2:1 complexation.

^{1}H NMR (400 MHz) titration experiments with **5** and **9** were performed on a Bruker DPX 400 FT-NMR spectrometer. The initial ^{1}H NMR spectrum was recorded, and aliquots of sodium perchlorate were added by microsyringe. After each addition and thorough mixing, the spectrum was recorded and changes in the chemical shifts of certain protons were noted. The computer program EQNMR[18] was used for data treatment and the stability constants were obtained from knowledge of the concentration of each component and the observed chemical shift for each data point.

CCDC-178442 (**1**), CCDC-178443 (**3**), and CCDC-178444 (**7a**) contain the supplementary crystallographic data for this paper. These data can be obtained free of charge via www.ccdc.can.ac.uk/conts/retrieving.html (or from the Cambridge Crystallographic Data Centre, 12 Union Road, Cambridge CB2 1EZ, UK; fax: (+44) 1223-336033; or deposit@ccdc.cam.uk).

Syntheses of platinum(II) complexes

[Pt(C^N^C)(Ph_2PB15C5)] (1): Ph_2PB15C5 (50 mg, 0.11 mmol) was added to a solution of [Pt(C^N^C)(dmso)] (50 mg, 0.10 mmol) in chloroform (10 mL). The resulting solution was stirred at room temperature under nitrogen for 2 h. Upon addition of *n*-hexane, yellow solids were obtained, and these were then filtered and dried. Recrystallization by layering of *n*-hexane onto a concentrated solution of **1** in dichloromethane gave the product as yellow crystals. Yield: 80 mg, 92%. ^{1}H NMR ($CDCl_3$): $\delta = 7.81$ (d, $J = 11.1$ Hz, 2H; $-PPh_2$), 7.79 (d, $J = 11.5$ Hz, 2H; $-PPh_2$), 7.64 (t, $J = 7.9$ Hz, 1H; dppy), 7.52 (dd, $J = 1.4$ Hz, $J' = 12.1$ Hz, 1H; $-C_6H_3-$), 7.35 (m, 11H; $-C_6H_3-$, $-PPh_2$, dppy), 6.91 (t, $J = 7.5$ Hz, 2H; dppy), 6.84 (dd, $J = 2.0$ Hz, $J' = 8.4$ Hz, 1H; $-C_6H_3-$), 6.69 (t, $J = 7.4$ Hz, 2H; dppy), 6.28 (d, $J = 7.5$ Hz, 2H; dppy), 4.14 (m, 2H; $C_6H_3OCH_2-$), 3.87 (m, 2H; $C_6H_3OCH_2-$), 3.70 ppm (m, 12H; $-OCH_2-$); ^{31}P{^{1}H} NMR ($CDCl_3$): $\delta = 29.0$ ppm (J(P,Pt) = 4082 Hz); positive-ion FAB-MS: m/z: 876 $[M]^+$; elemental analysis calcd (%) for $C_{43}H_{40}NO_5PPt$ (876): C 58.90, H 4.57, N 1.60; found: C 58.91, H 4.56, N 1.62.

[Pt(C^N^C)(Ph_2PDMP)] (2): The procedure was similar to that used for complex **1**, except that Ph_2PDMP (35 mg, 0.11 mmol) was used in place of Ph_2PB15C5. Yield: 72 mg, 97%. ^{1}H NMR ($CDCl_3$): $\delta = 7.82$ (d, $J = 11.6$ Hz, 2H; $-PPh_2$), 7.80 (d, $J = 11.6$ Hz, 2H; $-PPh_2$), 7.64 (t, $J = 7.9$ Hz, 1H; dppy),

0947-6539/02/0817-4074 $ 20.00+.50/0 *Chem. Eur. J.* **2002**, *8*, No. 17

7.59 (dd, $J = 1.8$ Hz, $J' = 12.4$ Hz, 1H; $-C_6H_3-$), 7.40 (m, 11H; $-C_6H_3-$, $-PPh_2$, dppy), 6.92 (t, $J = 7.4$ Hz, 2H; dppy), 6.88 (dd, $J = 2.3$ Hz, $J' = 8.0$ Hz, 1H; $-C_6H_3-$), 6.69 (t, $J = 7.4$ Hz, 2H; dppy), 6.28 (d, $J = 7.5$ Hz, 2H; dppy), 3.90 (s, 3H; $-OCH_3$), 3.50 ppm (s, 3H; $-OCH_3$); $^{31}P\{^1H\}$ NMR ($CDCl_3$): $\delta = 29.1$ ppm ($J(P,Pt) = 4082$ Hz); positive-ion FAB-MS: *m/z*: 746 $[M]^+$; elemental analysis calcd (%) for $C_{37}H_{30}NO_2PPt$ (746): C 59.52, H 4.02, N 1.88; found: C 59.49, H 4.01, N 1.86.

[Pt(C^N^C)(pyCOA15C5)] (3): The procedure was similar to that used for complex **1**, except that pyCOA15C5 (35 mg, 0.11 mmol) was used in place of Ph_2PB15C5. Yield: 70 mg, 94%. ^1H NMR ($CDCl_3$): $\delta = 9.12$ (d, $J = 6.6$ Hz, 2H; py), 7.53 (m, 3H; py, dppy), 7.46 (d, $J = 7.5$ Hz, 2H; dppy), 7.24 (d, $J = 8.7$ Hz, 2H; dppy), 7.19 (d, $J = 7.2$ Hz, 2H; dppy), 7.06 (t, $J = 7.5$ Hz, 2H; dppy), 6.93 (d, $J = 7.1$ Hz, 2H; dppy), 3.53–3.81 ppm (m, 20H; A15C5); IR (KBr): $\tilde{\nu} = 1651$ (ν(C=O)) cm^{-1}; positive-ion FAB-MS: *m/z*: 749 $[M]^+$; elemental analysis calcd (%) for $C_{33}H_{35}N_3O_5Pt$ (748): C 52.94, H 4.68, N 5.61; found: C 52.86, H 4.66, N 5.65.

[Pt(C^N^C)(pyCON($CH_2CH_2OCH_3$)$_2$)] (4): The procedure was similar to that used for complex **1**, except that pyCON($CH_2CH_2OCH_3$)$_2$ (26 mg, 0.11 mmol) was used in place of Ph_2PB15C5. Yield: 59 mg, 89%. ^1H NMR ($CDCl_3$): $\delta = 9.12$ (d, $J = 6.6$ Hz, 2H; py), 7.53 (m, 3H; py, dppy), 7.47 (d, $J = 7.7$ Hz, 2H; dppy), 7.26 (d, $J = 9.0$ Hz, 2H; dppy), 7.20 (d, $J = 7.2$ Hz, 2H; dppy), 7.08 (t, $J = 7.6$ Hz, 2H; dppy), 7.00 (d, $J = 7.1$ Hz, 2H; dppy), 3.73 (m, 4H; $-NCH_2-$), 3.60 (t, $J = 1.1$ Hz, 2H; $-CH_2OCH_3$), 3.53 (t, $J = 1.0$ Hz, 2H; $-CH_2OCH_3$), 3.41 (s, 3H; $-OCH_3$), 3.36 ppm (s, 3H; $-OCH_3$); IR (KBr): $\tilde{\nu} = 1650$ (ν(C=O)) cm^{-1}; positive-ion FAB-MS: *m/z*: 662 $[M]^+$; elemental analysis calcd (%) for $C_{29}H_{29}N_3O_3Pt$ (662): C 52.57, H 4.38, N 6.34; found: C 52.54, H 4.34, N 6.32.

[Pt(C^N^C)(pyC≡CB15C5)] (5): The procedure was similar to that used for complex **1**, except that pyC≡CB15C5 (40 mg, 0.11 mmol) was used in place of Ph_2PB15C5. Yield: 71 mg, 90%. ^1H NMR (CD_2Cl_2): $\delta = 8.98$ (dd, $J = 1.4$ Hz, $J' = 5.4$ Hz, 2H; py), 7.58 (t, $J = 7.9$ Hz, 1H; dppy), 7.51 (dd, $J = 1.5$ Hz, $J' = 5.4$ Hz, 2H; py), 7.48 (d, $J = 7.8$ Hz, 2H; dppy), 7.29 (d, $J = 8.0$ Hz, 2H; dppy), 7.25 (dd, $J = 1.8$ Hz, $J' = 8.3$ Hz, 1H; $-C_6H_3-$), 7.21 (dt, $J = 1.2$ Hz, $J' = 7.2$ Hz, 2H; dppy), 7.12 (d, $J = 1.8$ Hz, 1H; $-C_6H_3-$), 7.06 (dt, $J = 1.4$ Hz, $J' = 7.5$ Hz, 2H; dppy), 6.96 (d, $J = 7.1$ Hz, 2H; dppy), 6.90 (d, $J = 8.3$ Hz, 1H; $-C_6H_3-$), 4.19 (m, 4H; $C_6H_3OCH_2-$), 3.93 (m, 4H; $-OCH_2-$), 3.76 ppm (m, 8H; $-OCH_2-$); IR (KBr): $\tilde{\nu} = 2206$ (ν(C≡C)) cm^{-1}; positive-ion FAB-MS: *m/z*: 794 $[M]^+$; elemental analysis calcd (%) for $C_{38}H_{34}N_2O_5Pt$ (793): C 57.50, H 4.28, N 3.53; found: C 57.56, H 4.33, N 3.51.

[Pt(C^N^C)(pyC≡CDMP)] (6): The procedure was similar to that used for complex **1**, except that pyC≡CDMP (26 mg, 0.11 mmol) was used in place of Ph_2PB15C5. Yield: 60 mg, 91%. ^1H NMR (CD_2Cl_2): $\delta = 8.98$ (dd, $J = 1.4$ Hz, $J' = 5.4$ Hz, 2H; py), 7.58 (t, $J = 7.9$ Hz, 1H; dppy), 7.50 (dd, $J = 1.5$ Hz, $J' = 5.4$ Hz, 2H; py), 7.48 (d, $J = 7.8$ Hz, 2H; dppy), 7.30 (d, $J = 8.0$ Hz, 2H; dppy), 7.25 (dd, $J = 1.8$ Hz, $J' = 8.3$ Hz, 1H; $-C_6H_3-$), 7.20 (dt, $J = 1.2$ Hz, $J' = 7.2$ Hz, 2H; dppy), 7.12 (d, $J = 1.9$ Hz, 1H, $-C_6H_3-$), 7.06 (dt, $J = 1.4$ Hz, $J' = 7.5$ Hz, 2H; dppy), 6.98 (d, = 7.2 Hz, 2H; dppy), 6.91 (d, $J = 8.3$ Hz, 1H; $-C_6H_3-$), 3.91 (s, 3H; $-OCH_3$), 3.90 ppm (s, 3H; $-OCH_3$); IR (KBr): $\tilde{\nu} = 2204$ (ν(C≡C)) cm^{-1}; positive-ion FAB-MS: *m/z*: 663 $[M]^+$; elemental analysis calcd (%) for $C_{32}H_{24}N_2O_2Pt$ (663): C 57.92, H 3.62, N 4.22; found: C 57.90, H 3.64, N 4.21.

[Pt(trpy)(Ph_2PB15C5)](X)$_2$ (X = OTf 7a, PF_6 7b): Ph_2PB15C5 (65 mg, 0.14 mmol) was added to a suspension of [Pt(trpy)(MeCN)](OTf)$_2$ (100 mg, 0.13 mmol) in acetone. The reaction mixture turned from yellow to a clear orange solution and was stirred under nitrogen for 12 h at room temperature. Diffraction-quality crystals of **7a** were obtained by layering of petroleum ether onto a concentrated acetone solution of the complex. Alternatively, after metathesis reaction with Bu_4PF_6, orange solids of **7b** were collected in methanol by filtration, and were then air-dried. Subsequent recrystallization by layering of petroleum ether onto a concentrated acetone solution of the product gave **7b** as pale orange crystals. Yield: 125 mg, 82%. ^1H NMR (CD_3CN) for **7b**: $\delta = 8.62$ (t, $J = 8.1$ Hz, 1H; trpy), 8.46 (d, $J = 8.0$, 2H; trpy), 8.34 (d, $J = 8.0$, 2H; trpy), 8.26 (t, $J = 7.8$ Hz, 2H; trpy), 8.05 (m, 4H; trpy), 7.73 (m, 3H; $-PPh_2$), 7.59 (m, 4H; $-PPh_2$), 7.45 (m, 3H; $-PPh_2$), 7.23 (m, 2H; $-C_6H_3-$), 7.10 (dd, $J = 2.8$ Hz, $J' = 8.4$ Hz, 1H; $-C_6H_3-$), 4.17 (m, 2H; $C_6H_3OCH_2-$), 3.96 (m, 2H; $C_6H_3OCH_2-$), 3.82 (m, 2H; $-OCH_2-$), 3.71 (m, 2H; $-OCH_2-$), 3.65 (m, 2H; $-OCH_2-$), 3.59 ppm (m, 6H; $-OCH_2-$); $^{31}P\{^1H\}$ NMR (CD_3CN): $\delta = 16.0$ ($J(P,Pt) = 3627$ Hz); positive-ion ESI-MS: *m/z*: 1025 $[M - PF_6]^+$; elemental analysis calcd (%) for $C_{41}H_{40}F_{12}N_3O_5P_3Pt$ (1170): C 42.05, H 3.42, N 3.59; found: C 42.10, H 3.44, N 3.62.

[Pt(trpy)(Ph_2PDMP)](PF_6)$_2$ (8): The procedure was similar to that used for complex **7b**, except that Ph_2PDMP (46 mg, 0.14 mmol) was used in place of Ph_2PB15C5. Recrystallization by layering of petroleum ether onto a concentrated acetone solution of the product gave **8** as pale orange needles. Yield: 105 mg, 77%. ^1H NMR (CD_3CN): $\delta = 8.63$ (t, $J = 7.4$ Hz, 1H; trpy), 8.48 (d, $J = 7.7$ Hz, 2H; trpy), 8.38 (d, $J = 7.6$ Hz, 2H; trpy), 8.26 (t, $J = 7.9$ Hz, 2H; trpy), 8.07 (m, 4H; trpy), 7.74 (m, 3H; $-PPh_2$), 7.63 (m, 4H; $-PPh_2$), 7.42 (m, 3H; $-PPh_2$), 7.23(m, 2H; $-C_6H_3-$), 7.13 (dd, $J = 2.9$ Hz, $J' = 8.4$ Hz, 1H; $-C_6H_3-$), 3.90 (s, 3H; $-OCH_3$), 3.68 ppm (s, 3H; $-OCH_3$); $^{31}P\{^1H\}$ NMR (CD_3CN): $\delta = 16.0$ ppm ($J(P,Pt) = 3625$ Hz); positive-ion ESI-MS: *m/z*: 895 $[M - PF_6]^+$; elemental analysis calcd for $C_{35}H_{30}F_{12}N_3O_2P_3Pt$ (1040): C 40.38, H 2.88, N 4.04; found: C 40.32, H 2.87, N 4.06.

[Pt(trpy)(pyC≡CB15C5)](PF_6)$_2$ (9): The procedure was similar to that used for complex **7b**, except that pyC≡CB15C5 (53 mg, 0.14 mmol) was used in place of Ph_2PB15C5. Recrystallization by layering of petroleum ether onto a concentrated acetone solution of the product gave **9** as bright orange crystals. Yield: 100 mg, 71%. ^1H NMR ($(CD_3)_2CO$): $\delta = 9.35$ (d, $J = 6.8$ Hz, 2H; py), 8.78 (m, 5H; trpy), 8.64 (t, $J = 7.9$ Hz, 2H; trpy), 8.28 (d, $J = 6.8$ Hz, 2H; trpy), 8.07 (d, $J = 6.8$ Hz, 2H; py), 7.97 (m, 2H; trpy), 7.29 (dd, $J = 1.9$ Hz, $J' = 8.3$ Hz, 1H; $-C_6H_3-$), 7.23(d, $J = 1.9$ Hz, 1H; $-C_6H_3-$), 7.08 (d, $J = 8.4$ Hz, 1H; $-C_6H_3-$), 4.17 (m, 4H; $C_6H_3OCH_2-$), 3.87 (m, 4H; $-OCH_2-$), 3.69 ppm (m, 8H; $-OCH_2-$); IR (KBr): $\tilde{\nu} = 2205$ (ν(C≡C)) cm^{-1}; positive-ion ESI-MS: *m/z*: 942 $[M - PF_6]^+$; elemental analysis calcd (%) for $C_{36}H_{34}F_{12}N_4O_5P_2Pt$ (1087): C 39.74, H 3.13, N 5.15; found: C 39.75, H 3.16, N 5.10.

[Pt(trpy)(pyC≡CDMP)](PF_6)$_2$ (10): The procedure was similar to that used for complex **7b**, except that pyC≡CDMP (36 mg, 0.15 mmol) was used in place of Ph_2PB15C5. Recrystallization by layering of petroleum ether onto a concentrated acetone solution of the product gave **10** as orange crystals. Yield: 100 mg, 80%. ^1H NMR ($(CD_3)_2CO$): $\delta = 9.34$ (d, $J = 6.7$ Hz, 2H; py), 8.77 (m, 5H; trpy), 8.66 (t, $J = 7.9$ Hz, 2H; trpy), 8.29 (d, $J = 6.8$ Hz, 2H; trpy), 8.07 (d, $J = 6.8$ Hz, 2H; py), 7.99 (m, 2H; trpy), 7.30 (dd, $J = 1.9$ Hz, $J' = 8.2$ Hz, 1H; $-C_6H_3-$), 7.24 (d, $J = 2.0$ Hz, 1H; $-C_6H_3-$), 7.06 (d, $J = 8.3$ Hz, 1H; $-C_6H_3-$), 3.91 (s, 3H; $-OCH_3$), 3.85 (s, 3H; $-OCH_3$); IR (KBr): $\tilde{\nu} = 2205$ (ν(C≡C)) cm^{-1}; positive ESI-MS: *m/z*: 812 $[M - PF_6]^+$; elemental analysis calcd (%) for $C_{30}H_{24}F_{12}N_4O_2P_2Pt$ (957): C 37.62, H 2.51, N 5.85; found: C 37.64, H 2.53, N 5.88.

Crystal structure determination: All the experimental details are given in Table 1. Single crystals of **1** and **3** were obtained by layering of *n*-hexane onto concentrated dichloromethane solutions of the respective complexes. Crystals of **1** and **3** mounted in glass capillaries were used for data collection at 28°C on a MAR diffractometer with a 300 mm image plate detector using graphite monochromatized Mo-K_α radiation ($\lambda = 0.71073$ Å). The images were interpreted and intensities integrated by use of the program DENZO.[19] The structure was solved by direct methods with the aid of the SHELXS-97 program[20] on a PC. Pt atoms were located by direct methods. The positions of the other non-hydrogen atoms were found after successful refinement by full-matrix, least-squares with the SHELXL-97[21] program on a PC. The crystallographic asymmetric unit of **1** consists of two formula units: two molecules and two dichloromethane solvent molecules. In the final stage of least-squares refinement, all non-hydrogen atoms were refined anisotropically. For **3**, one crystallographic asymmetric unit also consists of two formula units. In the final stage of least-squares refinement, all atoms on the crown ether, C(17), and C(50) were refined isotropically, while the other non-hydrogen atoms were refined anisotropically.

Single crystals of **7a** were obtained by layering of petroleum ether onto a concentrated acetone solution of the complex. An orange crystal mounted in a glass capillary was used for data collection at 28°C on a Rigaku AFC7R diffractometer. The space group was determined on the basis of systematic absences and on a statistical analysis of intensity distribution and the successful refinement of the structure was solved by Patterson methods and expanded by Fourier methods (PATTY)[22] and refinement by full-matrix, least squares with the TeXsan[23] software package on a Silicon Graphics Indy computer. One crystallographic asymmetric unit consists of one formula unit. In the least-squares refinement, all 51 non-hydrogen atoms of the complex cation and 2S atoms were refined anisotropically, 22 non-hydrogen atoms of the anion and solvent

molecules were refined isotropically, and 52 H atoms at calculated positions with thermal parameters equal to 1.3 times that of the attached C atoms were not refined.

Acknowledgements

V.W.-W.Y. acknowledges support from the University of Hong Kong, Foundation for Educational Development and Research Limited, and the receipt of a Croucher Senior Research Fellowship (2000–2001) from the Croucher Foundation, and financial support from the Research Grants Council of the Hong Kong Special Administrative Region, China (Project No. HKU 7123/00P). R.P.-L.T. acknowledges the receipt of a postgraduate studentship, administered by the University of Hong Kong, and K.M.-C.W. the receipt of a University Postdoctoral Fellowship from the University of Hong Kong. Helpful discussions with Prof. V. M. Miskowski are gratefully acknowledged. Dr. M. J. Hynes is gratefully acknowledged for providing us with the EQNMR program.

[1] a) A. Vogler, H. Kunkely, *Top. Curr. Chem.* **2001**, *213*, 143–182; b) J. A. Zuleta, C. A. Chesta, R. Eisenberg, *J. Am. Chem. Soc.* **1989**, *111*, 8916–8917; c) H. Yersin, W. Humbs, J. Strasser, *Coord. Chem. Rev.* **1997**, *159*, 325–358; d) H. Yersin, D. Donges, *Top. Curr. Chem.* **2001**, *214*, 81–186; e) C. M. Che, K. T. Wan, L. Y. He, C. K. Poon, V. W. W. Yam, *J. Chem. Soc. Chem. Commun.* **1989**, 943–944; f) M. Hissler, A. Harriman, A. Khatyr, R. Ziessel, *Chem. Eur. J.* **1999**, *5*, 3366–3381.

[2] a) T. K. Aldridge, E. M. Stacy, D. R. McMillin, *Inorg. Chem.* **1994**, *33*, 722–727; b) R. Büchner, J. S. Field, R. J. Haines, *Inorg. Chem.* **1997**, *36*, 3952–3956; c) D. K. Crites Tears, D. R. McMillin, *Coord. Chem. Rev.* **2001**, *211*, 195–205; d) J. F. Michalec, S. A. Bejune, D. G. Cuttell, G. C. Summerton, J. A. Gertenbach, J. S. Field, R. J. Haines, D. R. McMillin, *Inorg. Chem.* **2001**, *40*, 2193–2200; e) V. W. W. Yam, R. P. L. Tang, K. M. C. Wong, K. K. Cheung, *Organometallics* **2001**, *20*, 4476–4482.

[3] S. F. Rice, H. B. Gray, *J. Am. Chem. Soc.* **1983**, *105*, 4571–4575; b) A. Lechner, G. Gliemann, *J. Am. Chem. Soc.* **1989**, *111*, 7469–7475; c) V. M. Miskowski, V. H. Houlding, *Inorg. Chem.* **1991**, *30*, 4446–4452; d) J. Biedermann, G. Gliemann, U. Klement, K. J. Range, M. Zabel, *Inorg. Chem.* **1990**, *29*, 1884–1888; e) J. A. Bailey, V. M. Miskowski, H. B. Gray, *Inorg. Chem.* **1993**, *32*, 369–370; f) W. B. Connick, L. M. Henling, R. E. Marsh, H. B. Gray, *Inorg. Chem.* **1996**, *35*, 6261–6265; g) S. W. Lai, M. C. W. Chan, K. K. Cheung, C. M. Che, *Inorg. Chem.* **1999**, *38*, 4262–4267; h) R. Büchner, C. T. Cunningham, J. S. Field, R. J. Haines, D. R. McMillin, G. C. Summerton, *J. Chem. Soc. Dalton Trans.* **1999**, *5*, 711–717; i) M. Hissler, W. B. Connick, D. K. Geiger, J. E. McGarrah, D. Lipa, R. J. Lachicotte, R. Eisenberg, *Inorg. Chem.* **2000**, *39*, 447–457; j) V. H. Houlding, V. M. Miskowski, *Coord. Chem. Rev.* **1991**, *111*, 145–152.

[4] a) J. J. Novoa, G. Aullón, P. Alemany, S. Alvarez, *J. Am. Chem. Soc.* **1995**, *117*, 7169–7171; b) W. B. Connick, R. E. Marsh, W. P. Schaefer, H. B. Gray, *Inorg. Chem.* **1997**, *36*, 913–922.

[5] a) S. J. Lippard, *Acc. Chem. Res.* **1978**, *11*, 211–217; b) Y. S. Wong, S. J. Lippard, *J. Chem. Soc. Chem. Commun.* **1977**, 824–825; c) K. W. Jennette, J. T. Gill, J. A. Sadownick, S. J. Lippard, *J. Am. Chem. Soc.* **1976**, *98*, 6159–6168; d) T. Ren, D. P. Bancroft, W. I. Sundquist, A. Masschelein, M. V. Keck, S. J. Lippard, *J. Am. Chem. Soc.* **1993**, *115*, 11341–11352; e) M. Cusumano, M. L. D. Pietro, A. Giannetto, *Inorg. Chem.* **1999**, *38*, 1754–1758; f) C. M. Che, M. Yang, K. H. Wong, H. L. Chan, W. Lam, *Chem. Eur. J.* **1999**, *5*, 3350–3356.

[6] a) C. Deuschel-Cornioley, T. Ward, A. von Zelewsky, *Helv. Chim. Acta.* **1988**, *71*, 130–133; b) M. Maestri, C. Deuschel-Cornioley, A. von Zelewsky, *Coord. Chem. Rev.* **1991**, *111*, 117–123; c) K. H. Wong, K. K. Cheung, M. C. W. Chan, C. M. Che, *Organometallics* **1998**, *17*, 3505–3511; d) W. Lu, M. C. W. Chan, K. K. Cheung, C. M. Che, *Organometallics* **2001**, *20*, 2477–2486.

[7] a) T. C. Cheung, K. K. Cheung, S. M. Peng, C. M. Che, *J. Chem. Soc. Dalton Trans.* **1996**, *8*, 1645–1651; b) S. W. Lai, M. C. W. Chan, T. C. Cheung, S. M. Peng, C. M. Che, *Inorg. Chem.* **1999**, *38*, 4046–4055; c) J. H. K. Yip, Suwarno, J. J. Vital, *Inorg. Chem.* **2000**, *39*, 3537–3543; d) S. W. Lai, H. W. Lam, W. Lu, K. K. Cheung, C. M. Che, *Organometallics* **2002**, *21*, 226–234.

[8] D. Song, Q. Wu, A. Hook, I. Kozin, S. Wang, *Organometallics* **2001**, *20*, 4683–4689.

[9] C. P. Newman, G. W. V. Cave, M. Wong, W. Erringto, N. W. Alcock, J. P. Rourke, *J. Chem. Soc. Dalton Trans.* **2001**, *18*, 2678–2682.

[10] a) G. W. V. Cave, N. W. Alcock, J. P. Rourke, *Organometallics* **1999**, *18*, 1801–1803; b) G. W. V. Cave, F. P. Fanizzi, R. J. Deeth, W. Errington, J. P. Rourke, *Organometallics* **2000**, *19*, 1355.

[11] a) P. R. Ashton, M. C. T. Fyfe, S. K. Hickingbottom, J. Fraser Stoddart, A. J. P. White, D. J. Williams, *J. Chem. Soc. Perkin Trans. 2* **1998**, *10*, 2117–2128; b) P. D. Beer, *Acc. Chem. Res.* **1998**, *31*, 71–80; c) A. P. de Silva, D. B. Fox, A. J. M. Huxley, N. D. McClengahan, J. Roiron, *Coord. Chem. Rev.* **1999**, *185–186*, 297–306; d) V. W. W. Yam, C. K. Li, C. L. Chan, *Angew. Chem. Int. Ed.* **1998**, *37*, 2857–2859; *Angew. Chem.* **1998**, *110*, 3041–3044; e) V. W. W. Yam, K. K. W. Lo, *Coord. Chem. Rev.* **1999**, *184*, 157–240; f) V. W. W. Yam, C. L. Chan, C. K. Li, K. M. C. Wong, *Coord. Chem. Rev.* **2001**, *216–217*, 173–194; g) J. L. Sessler, J. M. Davis, *Acc. Chem. Res.* **2001**, *34*, 989–997; h) Z. Naal, J. H. Park, S. Bernhard, J. P. Shapleigh, C. A. Batt, H. D. Abruna, *Anal. Chem.* **2002**, *74*, 140–148.

[12] V. W. W. Yam, R. P. L. Tang, K. M. C. Wong, C. C. Ko, K. K. Cheung, *Inorg. Chem.* **2001**, *40*, 571–574.

[13] G. Annibale, P. Bergamini, V. Beratolasi, M. Cattabriga, A. Lazzaro, A. Marchi, G. Vertuani, *J. Chem. Soc. Dalton Trans.* **1999**, *21*, 3877–3882.

[14] M. G. Colombo, H. U. Güdel, *Inorg. Chem.* **1993**, *32*, 3081–3087.

[15] T. Okano, M. Iwahara, H. Konishi, J. Kiji, *J. Organomet. Chem.* **1988**, *346*, 267–275.

[16] C. F. Martens, A. P. H. J. Schenning, M. C. Feiters, J. Heck, G. Beurskens, P. T. Beurskens, E. Steinwender, R. J. M. Nolte, *Inorg. Chem.* **1993**, *32*, 3029–3033.

[17] L. D. Ciana, A. Haim, *J. Heterocyclic. Chem.* **1984**, *21*, 607.

[18] M. J. Hynes, *J. Chem. Soc. Dalton Trans.* **1993**, 311–312.

[19] DENZO: " *The HKL Manual* - A description of programs DENZO, XDISPLAYF, and SCALEPACK" written by D. Gewirth with the cooperation of the program authors Z. Otwinowski and W. Minor, **1995**, Yale University, New Haven (US).

[20] SHELXS97: G. M. Sheldrick, SHELX97: Programs for Crystal Structure Analysis (Release 97–2), **1997**, University of Göttingen (Germany).

[21] SHELXL97: G. M. Sheldrick, SHELX97: Programs for Crystal Structure Analysis (Release 97–2), **1997**, University of Göttingen (Germany).

[22] PATTY: P. T. Beurskens, G. Admiraal, G. Beurskens, W. P. Bosman, S. Garcia-Granda, R. O. Gould, J. M. M. Smits, C. Smykalla, **1992**, The DIRDIF program system, Technical Report of the Crystallography Laboratory, University of Nijmegen, The Netherlands.

[23] TeXsan: Crystal Structure Analysis Package, Molecular Structure Corporation (**1985** and **1992**), The Woodlands, Texas (US).

Received: February 4, 2002 [F3849]

